Ligand activation leads to regulated intramembrane proteolysis of fibroblast growth factor receptor 3

Catherine R. Degnin[a], Melanie B. Laederich[a,b], and William A. Horton[a,c]
[a]Research Center, Shriners Hospital for Children, Portland, OR 97239; [b]Department of Cell and Developmental Biology and [c]Department of Molecular and Medical Genetics, Oregon Health and Science University, Portland, OR 97239

ABSTRACT **Fibroblast growth factor receptor 3 (FGFR3) is a major negative regulator of bone growth that inhibits the proliferation and differentiation of growth plate chondrocytes. Activating mutations of its c isoform cause dwarfism in humans; somatic mutations can drive oncogenic transformation in multiple myeloma and bladder cancer. How these distinct activities arise is not clear. FGFR3 was previously shown to undergo proteolytic cleavage in the bovine rib growth plate, but this was not explored further. Here, we show that FGF1 induces regulated intramembrane proteolysis (RIP) of FGFR3. The ectodomain is proteolytically cleaved (S1) in response to ligand-induced receptor activation, but unlike most RIP target proteins, it requires endocytosis and does not involve a metalloproteinase. S1 cleavage generates a C-terminal domain fragment that initially remains anchored in the membrane, is phosphorylated, and is spatially distinct from the intact receptor. Ectodomain cleavage is followed by intramembrane cleavage (S2) to generate a soluble intracellular domain that is released into the cytosol and can translocate to the nucleus. We identify the S1 cleavage site and show that γ-secretase mediates the S2 cleavage event. In this way we demonstrate a mechanism for the nuclear localization of FGFR3 in response to ligand activation, which may occur in both development and disease.**

Monitoring Editor
Jean E. Gruenberg
University of Geneva

Received: Jan 31, 2011
Revised: Aug 12, 2011
Accepted: Aug 18, 2011

INTRODUCTION

The fibroblast growth factor (FGF) receptors (FGFRs) comprise a family of four closely related receptor tyrosine kinases (RTKs), FGFR1–4. The family includes b and c isoforms of FGFR1–3, which are expressed primarily in epithelial and mesenchymal tissues, respectively. FGFR functions are best understood in the context of development. Genetic disturbances of FGFRs are responsible for a number of developmental disorders (Webster and Donoghue, 1997; Burke *et al.*, 1998); they also contribute to adult cancers (Bernard-Pierrot *et al.*, 2006; Chaffer *et al.*, 2007). Among the FGFRs, FGFR3 has received much attention as a key negative regulator of linear bone growth (Colvin *et al.*, 1996; Deng *et al.*, 1996a). Gain-of-function mutations of FGFR3 cause the most common forms of dwarfism in humans, including achondroplasia (ACH; Shiang *et al.*, 1994; Rousseau *et al.*, 1996a) and the more severe thanatophoric dysplasia types I and II (TDI/II; Tavormina *et al.*, 1995; Rousseau *et al.*, 1996b). In the skeletal growth plate, activating mutations in FGFR3 are believed to be antiproliferative. In contrast, similar somatic mutations have been detected in several neoplasias, including multiple myeloma (Chesi *et al.*, 1997; Richelda *et al.*, 1997), bladder cancer (Chaffer *et al.*, 2007), and cervical cancer (Cappellen *et al.*, 1999), where they are believed to drive proliferation and inhibit apoptosis (Trudel *et al.*, 2004).

Its importance to both development and disease has prompted interest in how FGFR3 propagates signals and how its signal output

This article was published online ahead of print in MBoC in Press (http://www.molbiolcell.org/cgi/doi/10.1091/mbc.E11-01-0080) on August 24, 2011.

Address correspondence to: William A. Horton (wah@shcc.org).

Abbreviations used: ACH, achondroplasia; ADAM, A disintegrin and metalloproteinase; Baf, bafilomycin A_1; CTD, C-terminal domain; DAPT, *N*-(*N*-(3,5-difluorophenacetyl)-L-alanyl)-*S*-phenylglycine *t*-butyl ester; ECD, extracellular domain; FGF, fibroblast growth factor; FGFR, fibroblast growth factor receptor; FRT, FLP-recombinase target; MβCD, methyl-β-cyclodextrin; MEF, mouse embryonic fibroblast; MMP, metalloproteinase; PM, plasma membrane; TD, thanatophoric dysplasia; TM, transmembrane domain; RIP, regulated intramembrane proteolysis; RTK, receptor tyrosine kinase; sICD, soluble intracellular domain; TGN, *trans*-Golgi network.

is regulated. Several pathways have been identified downstream of FGFR3. The ERK1/2, p38 MAPK, and STAT (especially STAT1) pathways appear to be most relevant to skeletal growth, whereas the RAS/MAPK, PLC-γ, and PI3K/AKT pathways have been implicated in cancer. Decreasing the duration of ERK1/2 activation has been correlated with switching FGFR3 signaling from growth arrest/differentiation (in chondrocytes and PC12 cells) to proliferation (in other cell types and cancer), but the cellular context mediating this switch is not understood (Dailey *et al.*, 2005).

Many membrane-bound, cell-surface proteins, including adhesion molecules, growth factors, and receptors, are proteolytically cleaved in or near the membrane in a regulated process commonly referred to as ectodomain shedding (S1 cleavage), which is often followed by constitutive cleavage within the transmembrane domain by an intramembrane cleaving protease such as γ-secretase (S2 cleavage). These sequential cleavage events are collectively referred to as regulated intramembrane proteolysis (RIP; Brown *et al.*, 2000; Kopan and Ilagan, 2004). Of the RTKs known to undergo ectodomain shedding, at least half have subsequently been shown to undergo S2 cleavage (Ancot *et al.*, 2009); more are likely to follow. S1 cleavage is usually mediated by one of two membrane-anchored metalloproteinases, A disintegrin and metalloproteinase (ADAM) 10 or 17. Cleavage occurs a short distance from the transmembrane domain, in the so-called extracellular stem region. The proteolytic activity of ADAM 10/17 is typically triggered by receptor activation, protein kinase C activation by phorbol esters such as phorbol-12-myristate-13-acetate (PMA), cytokine stimulation, and calcium influx (Blobel *et al.*, 2009). Ectodomain shedding can attenuate receptor signaling by down-regulating the number of receptors at the cell surface or by generating a soluble extracellular domain (ECD) that competes with surface-bound receptors for ligand binding (Ancot *et al.*, 2009). Ectodomain shedding can generate a membrane-anchored intracellular domain fragment that functions independent of the intact receptor, as has been described for TrkA (Diaz-Rodriguez *et al.*, 1999) and IL-2Rβ (de Oca *et al.*, 2010). It can also trigger RIP (S2 cleavage) to generate a soluble intracellular domain (sICD) with distinct properties, such as found with ErbB4 (Ni *et al.*, 2001; Williams *et al.*, 2004; Linggi *et al.*, 2006; Naresh *et al.*, 2006; Sardi *et al.*, 2006), Met (Pozner-Moulis *et al.*, 2006), Ryk (Lyu *et al.*, 2008), and p75 (Parkhurst *et al.*, 2010). The membrane-embedded γ-secretase complex primarily mediates S2 cleavage, although the Rhomboid and S2P family proteases are sometimes involved (Lal and Caplan, 2011). The γ-secretase complex consists of five proteins: presenilins 1 and 2, which harbor the catalytic sites of the complex (Wolfe, 2009); nicastrin, which mediates substrate binding by specifically recognizing the free N-terminal stub resulting from S1 cleavage (Shah *et al.*, 2005); and APH and Pen-2.

Whereas many transmembrane proteins undergo ectodomain shedding at the plasma membrane (PM), others are cleaved following endocytosis. For example, ErbB4 is shed from the PM in cells stimulated by PMA (Vecchi *et al.*, 1996), whereas ligand-activated ErbB4 must be endocytosed prior to cleavage (Zhou and Carpenter, 2000). ErbB4's ECD is found in the supernatant of PMA-stimulated cells; its fate following ligand activation is less well defined. Ectodomain cleavage of the transferrin receptor occurs after endocytosis and acts to prevent receptor recycling (Rutledge *et al.*, 1994). In another example, the Toll-like receptor 9 is endocytosed to an endolysosomal compartment, where it undergoes ectodomain cleavage by a cathepsin; cleavage is absolutely required for its activity (Park *et al.*, 2008). In many cases, cleavage of the receptor alters aspects of its function (Hadland *et al.*, 2004; Ancot *et al.*, 2009; Carpenter and Liao, 2009).

In contrast to the aforementioned proteins, FGFRs have received only modest attention in the context of ectodomain shedding. Levi *et al.* (1996) described ectodomain shedding of FGFR1 within a region typically targeted by ADAM sheddases. They implicated matrix metalloproteinase (MMP) 2 as the responsible sheddase and suggested that cleavage attenuates signaling by blocking recycling and producing an extracellular fragment that sequesters relevant ligands. Consistent with this hypothesis, Hanneken (2001) characterized soluble FGFR1 from circulating blood and identified FGFR1b and FGFR1c fragments that did not correlate with known FGFR1 splice variants but shared the common C-terminal residue identified by Levi *et al*. FGFR2 can undergo ectodomain shedding by ADAM 9 (Peduto *et al.*, 2005) or ADAM 15 (Maretzky *et al.*, 2009), although another protease may also be responsible. Similar to FGFR1, ectodomain shedding of FGFR2 generates a soluble ECD that may act as a decoy to down-regulate FGFR signaling (Peduto *et al.*, 2005). Ectodomain shedding of FGFR3 has been reported in the bovine growth plate (Pandit *et al.*, 2002). Western blots of lysates generated from distinct regions of the growth plate and probed using a panel of epitope-specific FGFR3 antibodies revealed not only intact FGFR3, but also N- and C-terminal domain fragments restricted to discrete regions of the growth plate. Although Pandit *et al.* suggested that FGFR3 may be cleaved within a glutamate-rich stretch of the stem region, the cleavage site and the protease were not identified. Indeed, no mechanism for promoting or regulating cleavage of any FGFR has been elucidated.

Using a biochemical and cell biological approach, we examine cleavage of FGFR3 and provide a mechanism for ligand-induced RIP of FGFR3. Unlike what has been previously described for FGFRs and most other RTKs, our observations suggest that cleavage of FGFR3 requires receptor activation and endocytosis but does not involve a metalloproteinase. We suggest independent trafficking of the membrane-anchored receptor fragment prior to S2 cleavage and show that S2 cleavage generates an sICD that can translocate to the nucleus. This is the first demonstration of an FGFR undergoing RIP.

RESULTS

FGFR3 is cleaved in stable and transfected Cos7 cells

We first observed structural modification of the FGFR3 ectodomain in Cos7 cells stably expressing the IIIc isoforms of wild-type (wt) FGFR3 and FGFR3 bearing mutations found in three members of the achondroplasia family of human dwarfism (TDII, K650E; ACH, G380R; and TDI, R248C), each tagged with C-terminal green fluorescent protein (GFP). Western blots probed for the GFP epitope revealed an anomalous band migrating at approximately 72 kDa for wt and mutant FGFR3 (Figure 1C, arrow). Detection with GFP suggested that this band corresponds to the C-terminal domain (CTD) of FGFR3, which was confirmed by mass spectroscopy and protein sequencing (Supplemental Figure S1B). Such a CTD could result from internal initiation of translation, alternate splicing, or proteolytic cleavage of the full-length receptor. To distinguish between these possibilities we first asked whether an N-terminal domain fragment could be detected. We inserted a V5 epitope downstream of the signal peptide of wtFGFR3-GFP to generate dual-tagged V5-FGFR3-GFP (Figure 1B), which was transiently expressed in Cos7 cells. Whole-cell lysates (Figure 1D, lane 3) or membrane fractions (Figure 1D, lanes 1 and 2) prepared from transfected cells were analyzed by Western blot using antibodies against the N- or C-terminal epitopes. Both intact and CTD FGFR3 were detected with the membrane fraction (Figure 1D, lane 1, IB: GFP), whereas the N-terminal domain was detected only in whole-cell lysates (Figure 1D, lane 3, IB: V5). These results are consistent with ectodomain cleavage of

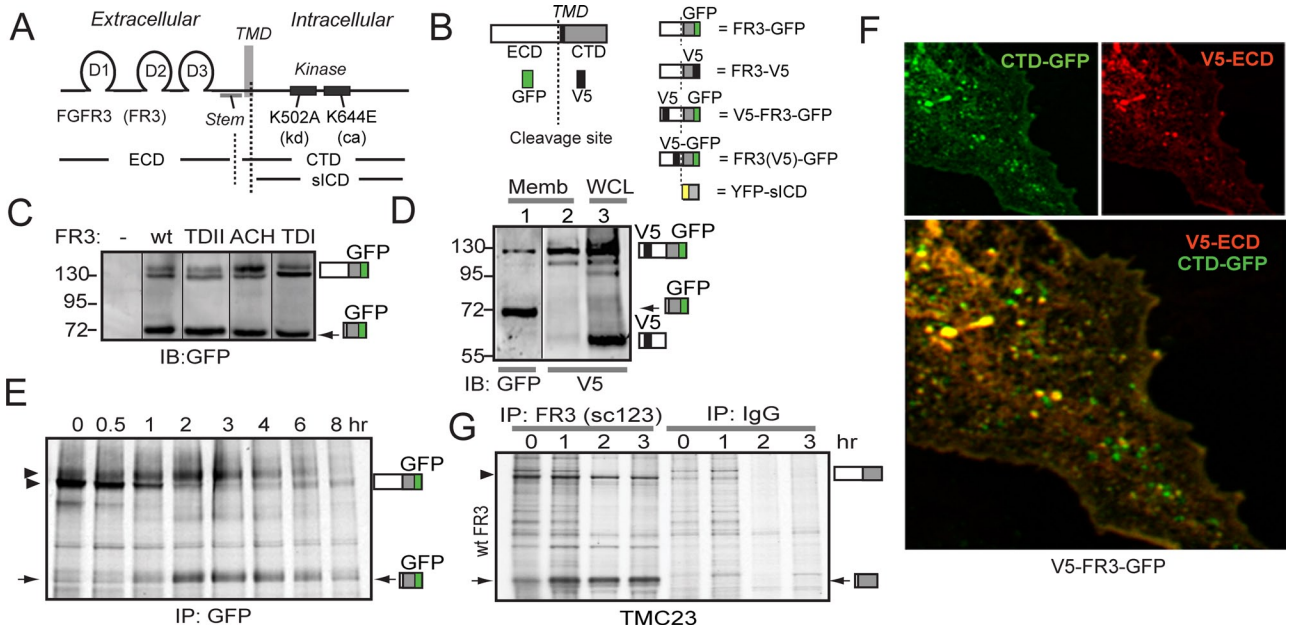

FIGURE 1: FGFR3 is proteolytically cleaved when expressed in the presence of serum. (A) Cartoon of relevant FGFR3 structures. D1–3: D-loops. CTD, C-terminal domain; ECD, extracellular domain; sICD, soluble intracellular domain; TMD, transmembrane domain. FR3, FGFR3. (B) Cartoon of FGFR3 constructs and epitope tags. (C–G) Arrow, cleaved FR3 CTD. (C) Western blot of control and Cos7 cell lysates stably expressing GFP-tagged wt and mutant FR3, probed for GFP epitope. Upper bands, intact receptor. (D) Membrane extracts (lanes 1, 2) and whole-cell lysates (WCL) (lane 3) prepared from Cos7 cells transiently expressing V5-FR3-GFP, probed for GFP (lane 1) or V5 (lanes 2, 3). (E) Pulse-chase analysis of Cos7 cells stably expressing wtFR3-GFP, immunoprecipitated for the GFP epitope. Arrowheads, mature FR3. (F) Confocal analysis of V5-FR3-GFP transiently expressed in Cos7 cells. Green, C-terminal GFP; red, N-terminal V5; yellow, colocalized epitopes. (G) Endogenous FGFR3 is cleaved. Pulse-chase analysis of TMC-23 cells immunoprecipitated for FGFR3 (sc123) or control immunoglobulin G.

FGFR3 such that the CTD retains the transmembrane domain (TMD) and the N-terminal ECD is released from the membrane.

To definitively show that FGFR3 is cleaved, Cos7 cells stably expressing wtFGFR3-GFP were pulse labeled using [^{35}S]methionine and chased in growth media. Lysates were affinity purified using an antibody against the C-terminal GFP epitope (Figure 1E). During the 45-min pulse FGFR3 matured from a high-mannose to the fully glycosylated mature receptor (arrowheads). Between 1 and 2 h of chase, a new band at approximately 72 kDa (arrow) was generated, coinciding with the maturation and subsequent loss of the intact receptor. Because this novel protein band appeared during the chase period, we conclude that it must have resulted from cleavage of the intact receptor.

To localize the cleavage products in intact cells, V5-FGFR3-GFP was transiently expressed in Cos7 cells, permeabilized, immunostained for the N-terminal V5 epitope, and imaged using confocal microscopy. Fluorescence from the C-terminal GFP (Figure 1F, green) produced a characteristic vesicular pattern in the cytoplasm of transfected cells (Cho *et al.*, 2004); the N-terminal V5 epitope produced a similar pattern (Figure 1F, red). When the images were merged many of the vesicles displayed colocalization (yellow), suggestive of intact FGFR3 or close proximity of the cleavage products. Many other vesicles fluoresced green, indicating the presence of only the membrane-anchored C-terminal fragment and suggesting that following proteolytic cleavage the CTD may traffic to a compartment distinct from the intact receptor. When primary chondrocytes were transfected we detected not only green-only vesicles, but also a number of red-only vesicles, suggesting independent trafficking and possibly increased stability of the ECD in these cells (Supplemental Figure S2A).

To determine whether ectodomain cleavage of FGFR3 is restricted to specific cell types, we tested several cell lines for cleavage of transiently expressed wtFGFR3-GFP under growth conditions. HeLa, 293T, HT1080, and mouse embryonic fibroblast (MEF) cells cleaved exogenous FGFR3, as was detected in Cos7 cells (Supplemental Figure S2B), whereas Chinese hamster ovary cells did not (Supplemental Figure S2C). To exclude the possibility that the C-terminal GFP tag contributes to cleavage, it was replaced by V5-His or mCherry, and the tagged receptors were transiently expressed in Cos7 or 293T cells (Supplemental Figure S2D); these proteins also generated a cleaved fragment that migrated at the position expected for the epitope-tagged CTD. Likewise, untagged FGFR3 was cleaved in transiently transfected 293T cells that were subject to pulse-chase analysis and immunoprecipitated using a C-terminal FGFR3 antibody (Supplemental Figure S2E).

Next we examined TMC23, a prechondrocytic mouse cell line that endogenously expresses FGFR3. Owing to the low level of endogenous FGFR3 expression, cells were subject to an extended pulse labeling in [^{35}S]methionine. Pulse-chase analysis using an antibody to the C-terminus of FGFR3, but not the immunoglobulin control, showed accumulation of the CTD during the chase period, excluding the possibility that cleavage of FGFR3 is an artifact of exogenous overexpression (Figure 1G). Thus, endogenous FGFR3 was also cleaved in an appropriate cell type.

Ectodomain cleavage requires receptor activation

For cleavage to play a role in modulating FGFR3 function we expect it to be regulated. FGFR3-induced signaling and phosphorylation could not be suppressed in serum-starved Cos7 cells stably expressing FGFR3, and receptor cleavage appeared to be constitutive. This

suggests that Cos7 cells may express endogenous FGFs that constitutively activate FGFR3. Therefore, to directly address the mechanism for FGFR3 cleavage, we developed stable, inducible FGFR3 expression lines using the T-Rex 293 cell line system containing the tetracycline (tet) repressor and a single FLP-recombinase target (FRT) site. This system allows for stable integration of a single FGFR3 copy within a distinct genetic locus. Protein is expressed only in the presence of tet, thus reducing complications from cellular adaptation to misexpressed FGFR3. When serum starved, these cells undergo growth arrest and exhibit minimal FGFR3 phosphorylation, and ERK signaling is suppressed. Unless otherwise stated, all remaining experiments were performed with these cell lines. FGFR3 cell lines carrying the C-terminal GFP and V5 epitopes generated similar results. For Western blots the smaller V5 epitope was used; when proteins were affinity purified or imaged, GFP was used.

Pulse-chase analysis of T-Rex 293 cells expressing wtFGFR3-GFP under growth conditions showed that the CTD derived from wtFGFR3 accumulated after 2 h of chase (Figure 2A, arrow). To determine whether an activated receptor is required for cleavage, wtFGFR3 cleavage was compared with constitutively active (ca) FGFR3 and a mutant that was unable to be activated, that is, kinase dead (kd). The K650E human TDII mutation known to constitutively activate the kinase (Webster and Donoghue, 1996) was used as caFGFR3, and the K502A mutation documented to abolish kinase activity was used as kdFGFR3 (Monsonego-Ornan *et al.*, 2002). The ca mutant was cleaved, whereas the kd mutant was not, suggesting that cleavage requires an activated receptor.

In support of cleavage requiring receptor activation, wtFGFR3 was not cleaved in cells that had been serum starved (0 h), but the CTD was detected within 1 h of FGF1 addition (Figure 2B, arrow). In contrast, caFGFR3 was cleaved both in the absence and presence of FGF1, and cleavage of kdFGFR3 was not detected under either condition (Figure 2B, bottom, longer exposure). To confirm these findings, cells expressing wtFGFR3 were treated with FGF1 in the absence or presence of FGFR kinase inhibitor PD173074 or SU5402 (Figure 2C). Ligand-induced cleavage was blocked by both low and high concentrations of PD173074 and attenuated by high concentrations of SU5402. The asterisk indicates a nonspecific band, which was also detected in the no-tet control lane.

Because wtFGFR3 is cleaved in response to ligand addition, it is likely that cleavage requires receptor expression at the PM. This was confirmed by showing that FGF1-induced cleavage was blocked when wtFGFR3 was trapped intracellularly using thapsigargin or tunicamycin (which inhibits exit from the endoplasmic reticulum [ER]), brefeldin A (which blocks anterograde transport from the Golgi; Figure 2D, top, left), or a temperature block (which inhibits exit from the *trans*-Golgi network (TGN; Figure 2E). Because of reports that caFGFR3 becomes activated in the ER (Lievens and Liboi,

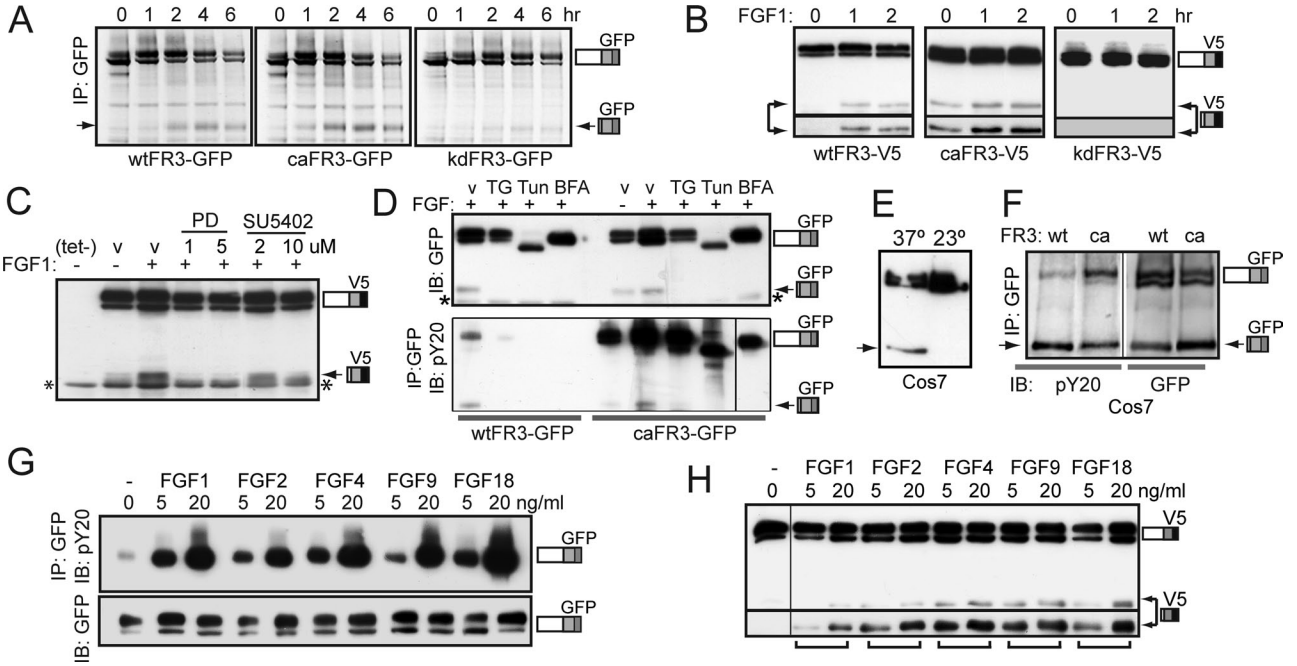

FIGURE 2: FGF1-induced cleavage requires FGFR3 activation. (A–H) Arrow, cleaved FR3; asterisk, nonspecific band. (A) Pulse-chase analysis of T-Rex 293 cell lines stably expressing wt, ca, or kdFR3-GFP in growth media, immunoprecipitated for GFP epitope. (B–D) Western blots of wtFR3-expressing T-Rex 293 cells, cultured in DMEM/FBS(–) media in the presence or absence of FGF1 and probed for C-terminal V5 epitope, unless stated otherwise. (B) Serum-starved cells activated with FGF1 for the times indicated. Bottom, longer exposure to show that kd receptor is not cleaved. (C) Cells treated 8 h with or without tet/FGF1, ± PD173074 (PD), or SU5402 as indicated. v, vehicle (dimethyl sulfoxide [DMSO]). (D) Cells cultured 8 h in the presence or absence of inhibitor as indicated. BFA, 6 μg/ml brefeldin A; TG, 1 mg/ml thapsigarin; Tun, 1 μg/ml tunicamycin; v, DMSO. Top, 1/10 WCL, probed for GFP. Bottom, IP GFP, IB phosphotyrosine (pY20). wtFR3, left; caFR3, right. (E) Western blot of Cos7 cells stably expressing wtFR3-GFP cultured 5 h at 37°C (left) or 23°C (right), probed for GFP. (F) Western blot of Cos7 cells stably expressing wt or caFR3-GFP cultured under growth conditions, immunoprecipitated for GFP and probed for phosphotyrosine (pY20, left). WCL 1/10 probed for GFP (right). (G) Serum-starved wtFR3-GFP expressing T-Rex 293 cells, activated 5 min with the growth factors indicated. Equal micrograms of lysate were immunoprecipitated for GFP and probed for phosphotyrosine (pY20). WCL 1/10 was probed for GFP (bottom, IB GFP). (H) T-Rex 293 cells expressing wtFR3 were tet induced for 8 h in DMEM/FBS(–) media containing the FGF species indicated. Western blot of lysates probed with V5 antibodies. Bottom, longer exposure to show relative amounts of cleaved FR3.

2003), we asked whether biosynthesis inhibitors also prevent caFGFR3 cleavage. As anticipated, caFGFR3 was phosphorylated in the presence of biosynthesis inhibitors but was not cleaved (Figure 2D, right lanes). These results suggest that FGFR3 activation is necessary but not sufficient for receptor cleavage.

Consistent with cleavage occurring after receptor activation, both intact and cleaved FGFR3 are phosphorylated in the presence of FGF1 (Figure 2D, bottom). Phosphorylation of the CTD was also observed in Cos7 cells stably expressing wt or caFGFR3 cultured under growth conditions. A significant portion of phosphorylated FGFR3 was attributed to the CTD (Figure 2F, left, IP GFP; IB pY20), suggesting that the CTD may contribute to FGFR3-mediated signaling.

Because FGFR3 activation is required for receptor cleavage and because some FGF ligands can induce distinct receptor responses under different cellular contexts (Belleudi *et al.*, 2007), we asked whether cleavage is an FGF1-specific or a general FGF-mediated phenomenon. Given that FGF receptors exhibit ligand specificity, we first confirmed that FGF1, FGF2, FGF4, FGF9, and FGF18 promote wtFGFR3 phosphorylation. After 5 min of exposure to ligand, the intensity of FGFR3 tyrosine phosphorylation was dependent on the concentration of the ligand (Figure 2G, top). We next observed that wtFGFR3 was cleaved in a ligand concentration–dependent manner (Figure 2H, bottom, longer exposure). In addition to ligand-induced cleavage, several RTKs are also cleaved in response to external stimuli such as phorbol esters. Similar to ErbB4, wtFGFR3 was cleaved following the addition of PMA but not ionomycin (Supplemental Figure S3A). In contrast, PMA did not exhibit cleavage of FGFR3 expressed in Chinese hamster ovary cells (Supplemental Figure S3B).

FGFR3 cleavage requires clathrin/dynamin–mediated endocytosis

To determine whether cleavage of FGFR3 occurs at the PM (i.e., shedding) or requires receptor endocytosis, we serum starved cells, blocked endocytosis, and then assayed for FGF1-induced cleavage. wtFGFR3-V5 was not cleaved when cells were pretreated with a hypertonic sucrose solution, which disrupts the clathrin lattice (Idkowiak-Baldys *et al.*, 2006), or with dynasore, which inhibits dynamin-mediated endocytosis (Macia *et al.*, 2006; Figure 3A). Methyl-β-cyclodextrin (MβCD), which disrupts lipid raft formation (Idkowiak-Baldys *et al.*, 2006), and filipin, which inhibits both raft- and caveolae-mediated endocytosis (Schnitzer *et al.*, 1994), failed to block receptor cleavage. In some contexts MβCD treatment can promote ectodomain shedding of selected substrates (Matthews *et al.*, 2003; von Tresckow *et al.*, 2004). This is not the case for FGFR3 (Supplemental Figure S3C). These data are consistent with cleavage of FGFR3 requiring endocytosis in a clathrin/dynamin–mediated process. To further document that inhibition of cleavage coincides with trapping FGFR3 at the PM, serum-starved cells were treated with FGF1 in the presence or absence of inhibitors, cell surface biotinylated at the times indicated, and precipitated with NeutrAvidin Gel. Whereas wtFGFR3 was cleared from the PM in FGF1-induced cells (rendering it inaccessible to the biotinylation reagent), the receptor was retained at the PM in the presence of kinase inhibitors or sucrose (Supplemental Figure S3D). To establish that sucrose inhibits endocytosis but not receptor phosphorylation, cells expressing wtFGFR3 were activated with FGF1 in the presence or absence of sucrose, immunoprecipitated using the GFP epitope, and immunoblotted for phosphotyrosine. As expected, sucrose treatment did not disrupt receptor phosphorylation (Supplemental Figure S3E).

Because cleavage of FGFR3 appears to require endocytosis, we asked how rapidly FGFR3 is endocytosed and whether this

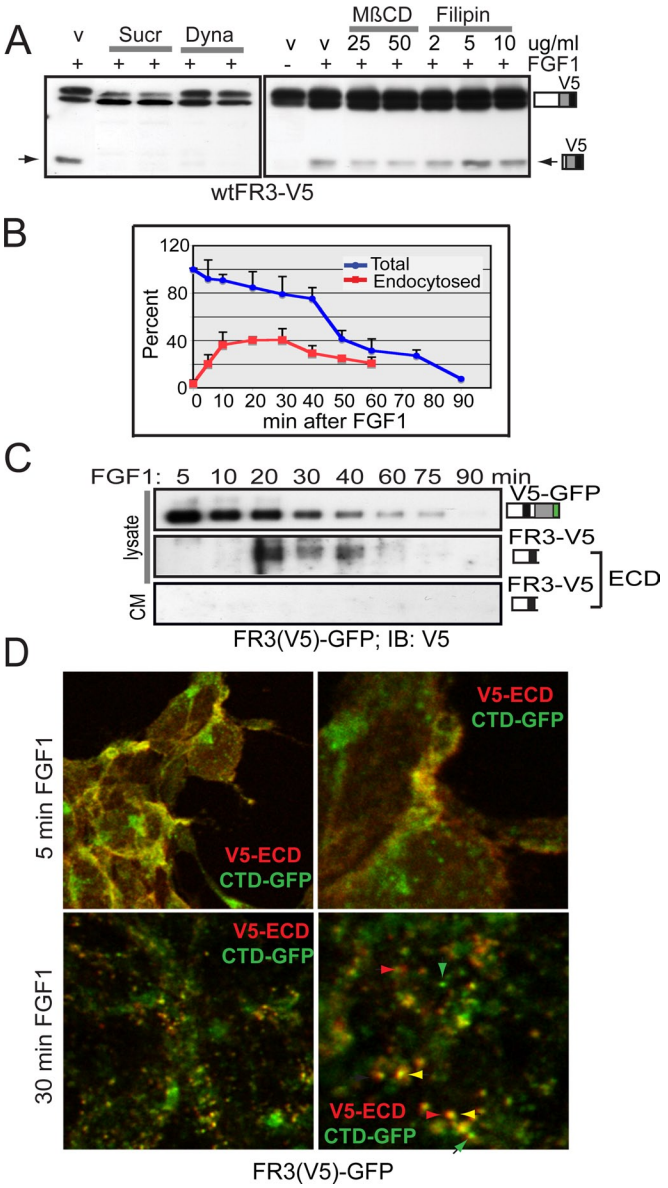

FIGURE 3: Endocytosis is required for FGF1-induced cleavage of FGFR3. (A) Western blot of lysates from wtFR3-V5–expressing T-Rex 293 cells induced 3 h ± FGF1 before treating an additional 5 h with drug or DMSO (v). Dyna, 67, 80 μM dynasore; MβCD, methyl-β-cyclodextrin; Sucr, 0.4 M sucrose. (B) Graphical analysis of three independent experiments plotting loss of intact cell surface biotinylated receptor (blue line) and endocytosis of intact, cell surface biotinylated, glutathione-resistant receptor (red line). SDs are given as error bars. (C) FR3(V5)-GFP expressing cells were serum starved, cell surface biotinylated, and then treated with FGF1 for the times indicated. Equal micrograms of lysate or all the culture media (CM) was affinity purified using NeutrAvidin Gel. Western blot using equal volumes of purified lysate or one half of purified CM was probed for N-terminal V5 epitope (ECD). ECD was detected by overexposing blots. (D) Serum-starved FR3(V5)-GFP–expressing cells were surface labeled with V5 antibodies, then stimulated with FGF1 to promote receptor internalization. Cells were fixed, permeabilized, probed with secondary antibodies (Alexa 543) to the endocytosed V5 epitope, and imaged by confocal microscopy. Right, higher-magnification image of left. Green, C-terminal GFP; red, endocytosed ECD-V5. Green arrowheads, GFP-containing vesicles; red arrowheads, ECD-containing vesicles; yellow arrowhead, colocalized ECD/CTD.

correlates with receptor cleavage. Serum-starved cells were subjected to cell surface biotinylation using a thiol-sensitive form of biotin. Cells were then incubated with prewarmed, FGF1-containing media and the loss (degradation plus cleavage) of total biotin-labeled receptor was evaluated (Figure 3B, blue line). In parallel, cell surface biotinylated cells were subjected to thiol cleavage of the PM-retained proteins following FGF1 addition, to assay the fraction of intact, biotin-labeled receptor that had been endocytosed and thus protected from the reducing agent (Figure 3B, red line). Results are shown graphically as the average of four independent experiments in which FGFR3 endocytosis peaks between 10 and 30 min of FGF1 addition. Because this assay cannot distinguish between cleaved or degraded FGFR3, we designed a dual-tagged receptor in which the V5 epitope was inserted N-terminal to the stem region near the D3 loop:stem junction (Figure 1B, FGFR3(V5)-GFP) and is retained with the ECD following receptor cleavage. Cells stably expressing FGFR3(V5)-GFP were serum starved, cell surface biotinylated, treated with FGF1, and cultured for the times indicated. The culture media and cell lysates were precipitated using NeutrAvidin Gel; Western blots were probed for the V5 (ECD) epitope. As is depicted graphically in Figure 3B, the intact, surface-labeled receptor was lost within 90 min of FGF1 addition (Figure 3C, top). On prolonged exposure the ECD was detected in cell lysates between 20 and 40 min of FGF1 addition, following receptor endocytosis (Figure 3C, middle) but was not detected in the culture media (Figure 3C, bottom).

We asked whether we could detect the segregation of cleaved, endocytosed receptor by confocal microscopy. Cells stably expressing FGFR3(V5)-GFP were serum starved and surface FGFR3 was labeled using anti-V5 antibodies. FGF1 was added, and cells were cultured for 5 or 30 min before cells were fixed, permeabilized, and stained using secondary antibodies against the endocytosed V5-ECD epitope. At 5 min the ECD and CTD colocalized (yellow) at the cell surface, whereas at 30 min discrete vesicles containing only ECD (red), CTD (green), or intact receptor (yellow) were detected (Figure 3D). GFP labels the receptor in both the biosynthetic and endocytic pathways.

Supplemental Figure S3A shows that PMA also promotes cleavage of FGFR3. If FGFR3 acts similar to other RTKs, FGFR3 should be cleaved immediately following PMA stimulation (Vecchi and Carpenter, 1997). Cleavage of FGFR3 was detected within 5 min of PMA addition to serum-starved cells (Supplemental Figure S3F), much sooner than cleavage induced by FGF1. This suggests that FGF1 and PMA may promote FGFR3 cleavage through distinct mechanisms.

FGFR3 cleavage involves endosomal cathepsins

A number of proteolytic enzymes could be responsible for ectodomain cleavage of FGFR3 following receptor activation. To narrow the possibilities, we tested general inhibitors of four of the five major classes of proteases at a range of concentrations (Overall and Blobel, 2007). We started with inhibitors of MMPs because the ectodomain sheddases ADAM10 and 17 were considered strong candidates for FGFR3 cleavage. Figure 4A shows that three general inhibitors of MMP/ADAM/ADAMTS proteinases (EDTA, BB94 and GM6001) failed to inhibit FGFR3 cleavage. Similar results were found using the small molecule, broad-spectrum MMP inhibitor marimastat (Supplemental Figure S4A, left). These results argue strongly against the involvement of ADAM10 or 17 sheddases in FGFR3 cleavage. Because FGF1 and PMA appear to promote cleavage of FGFR3 through distinct mechanisms, we asked whether MMP inhibitors could block PMA-induced cleavage. Surprisingly, they did not inhibit PMA-induced cleavage of FGFR3 (Supplemental Figure S4A, right), whereas they did block PMA-induced cleavage of ErbB4 (Supplemental Figure S4B).

Screening with general inhibitors for serine (AEBSF), cysteine (E64d), and aspartate (pepstatin A) proteases revealed that only AEBSF consistently blocked cleavage of FGFR3 in a dose-dependent manner (Figure 4B). We tested four additional serine protease inhibitors: aprotinin, antipain, chymostatin (Figure 4C), and leupeptin (not shown). Surprisingly, none inhibited cleavage of FGFR3.

On the basis of evidence that cleavage occurred following endocytosis of FGFR3, we next tested inhibitors of cathepsins, which typically act in the endosomal/lysosomal pathway. Several cathepsin inhibitors suppressed cleavage of FGFR3, including cathepsin inhibitor I (CpsI) and FA-FMK, which selectively inhibit cathepsins B, L, and S (Figure 4D). The cathepsin B inhibitor ca-074-me suppressed cleavage to a lesser extent in some, but not all, experiments.

Early endosomes undergo progressive acidification when fusing with, or maturing into, late endosomes/lysosomes, and proteases that act in this pathway typically have pH optima in the acidic range. If FGFR3 is cleaved in this pathway, then agents such as bafilomycin A_1 (Baf) that interfere with endo/lysosomal acidification should attenuate cleavage. Figure 4E shows that Baf treatment blocked FGF1-induced cleavage of FGFR3. Baf also increased the stability of the intact receptor, which is expected since lysosomal degradation was also blocked by deacidification.

FGFR3 is cleaved in the stem region

Pandit *et al.* (2002) proposed that FGFR3 is cleaved within a stretch of acidic residues in the FGFR3 stem region (and our membrane fractionation supports this possibility; Figure 1D). To further define the requirements for cleavage of FGFR3, stem region mutants (mFGFR3) were constructed and stable tet-inducible cell lines were established. The mutations and relative fraction of cleaved FGFR3 from at least three-independent experiments are summarized in Figure 5A. Most mutations that removed the LME amino acid motif (boxed) suppressed cleavage, whereas partial deletion, scrambling, or removing residues more proximal to the TMD did not. The epithelial FGFR3b isoform that retains the LME motif was cleaved like the c isoform (Supplemental Figure S5A, asterisk). Consistent with these observations, we identified a cleavage site within the LME motif by N-terminal sequencing (Figure 5B, arrow; sequenced residues are underlined). A homology search found that these sequences were not absolutely conserved between species, that is, the sequence is LVE in human and

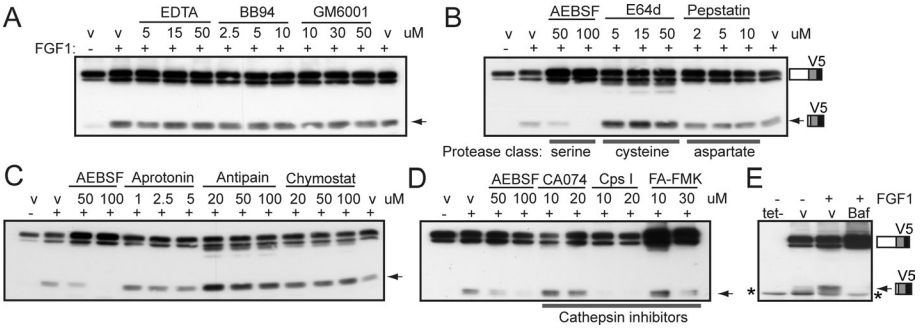

FIGURE 4: FGFR3 cleavage involves endosomal cathepsins. (A–E) wtFR3-V5–expressing T-Rex 293 cells treated with tet/FGF1, ± inhibitor, or DMSO (v), as indicated. Western blot of lysates probed for the V5 epitope. Arrow, cleaved FR3; asterisk, nonspecific band. Baf, 250 μM bafilomycin A_1; Chymostat, chymostatin; Cps I, cathepsin inhibitor I.

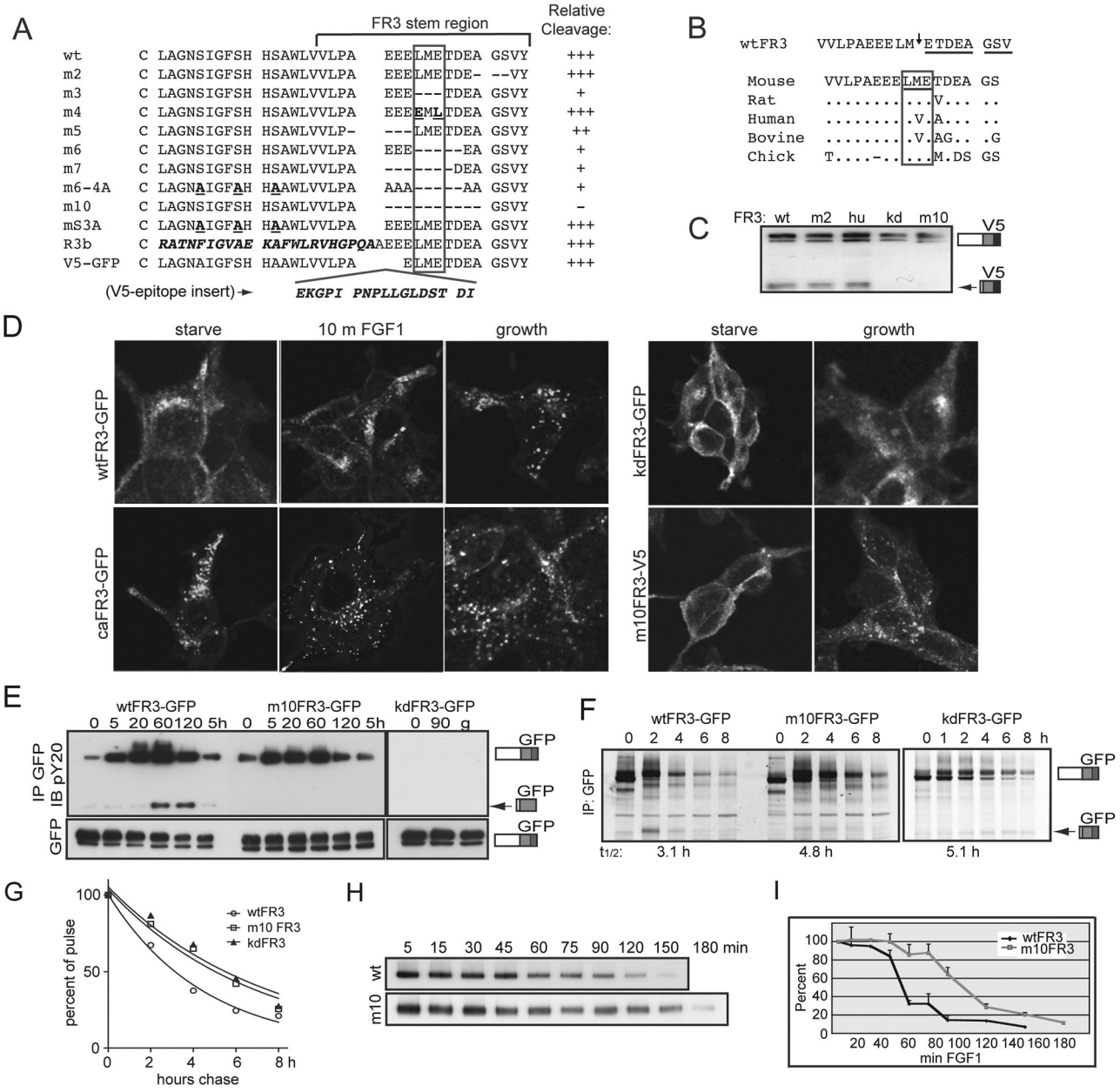

FIGURE 5: Disrupting cleavage alters the half-life, but not the trafficking, of FGFR3. (A–I) T-Rex 293 stable cell lines. Arrow, cleaved FR3. (A) Stem region sequence of mutants (m) generated and relative degree of cleavage, averaged from at least three independent experiments. Cell lines were tet-induced 8 h in the presence of FGF1; cleavage was assessed by Western blot using V5 or GFP epitope. +++, wt cleavage; ++, reduced cleavage; +, minimal cleavage; −, no cleavage detected. Putative cleavage region is boxed. Mutated residues are shown in bold; FR3b-specific sequence and V5 epitope insertion are shown in bold and italicized. (B) Top, cleavage site determined by N-terminal sequencing of gel-purified 72-kDa fragment. Arrow, cleavage site. Sequenced residues are underlined. Bottom, homology of cleavage region between species. Residues surrounding cleavage site are boxed; distinct amino acids are listed. (C) Representative Western blot of various stable FR3-V5 cell lines probed for V5 epitope. hu, human stem region. (D) Confocal images of wt and mutant FR3 following serum starvation, 10 min FGF1 addition, or cultured in growth media. GFP imaged directly; V5 probed with V5 antibody and Alexa 488 secondary antibody. (E) Cells expressing wt and mutant FR3-GFP were serum starved and then treated with FGF1 for the times indicated. Equal micrograms of lysates were immunoprecipitated for GFP and probed for phosphotyrosine (pY20). (F) Cells expressing wt, m10, and kdFR3-GFP were subject to pulse-chase analysis in the presence of FGF1 and immunoprecipitated for GFP. Arrow, cleaved FR3. T1/2, half-life of intact receptor calculated using GraphPad (La Jolla, CA). (G) Graphical depiction of the half-life for intact wt, m10, and kdFR3. (H) Cells expressing wt or m10FR3-V5 were serum starved, cell surface biotinylated, and stimulated with FGF1 for the times indicated. Equal micrograms of lysate were immunoprecipitated using NeutrAvidin Gel; the stability of the intact receptor was assessed by Western blot using the V5 epitope. (I) Graphical analysis of three independent experiments assaying loss of intact cell surface biotinylated receptor. SDs are shown as error bars.

bovine FGFR3, where cleavage was previously reported. We substituted the human stem region sequence into the mouse receptor to generate the huFGFR3 species and detected cleavage comparable to that of the murine wtFGFR3 (Figure 5C). We next focused on m10FGFR3, which suppresses cleavage when stably expressed in T-Rex 293 (Figure 5C, m10FGFR3) and MEF cells (Supplemental Figure S5B).

It is possible that mutation of the stem region alters receptor trafficking and that the impact on cleavage is secondary to mislocalization of the receptor. To address this possibility, we assessed trafficking of wt and mFGFR3 by confocal microscopy. Cells were serum-starved or cultured under growth conditions, fixed, and imaged (Figure 5D). wtFGFR3 was distributed in a diffuse to vesicular pattern throughout the cytosol in serum-starved cells but was more intense adjacent to the PM. This diffuse fluorescence coalesced into more discrete vesicles within 10 min of FGF1 treatment. In the presence of serum, wtFGFR3 displayed the characteristic punctate, vesicular pattern previously described for Cos7 cells under similar conditions (Cho *et al.*, 2004). These observations suggest that ligand activation of FGFR3 stimulates its movement from the surface of serum-starved cells into internal vesicular structures, a pattern that is stabilized under growth conditions in which stimulation is constant. As such, one would expect caFGFR3 to display the distinct vesicular pattern and kdFGFR3 to exhibit the diffuse PM pattern under all conditions. These expectations were confirmed. We next examined trafficking of m10FGFR3. Under serum-starvation conditions m10FGFR3 was detected near the PM in a diffuse pattern, whereas under growth conditions the receptor was found in a more discrete vesicular pattern, similar to wtFGFR3.

Because m10FGFR3 traffics normally and the deletion was generated outside of the ligand-binding domain, we anticipated that this mutation would have no impact on receptor phosphorylation. This was confirmed in experiments in which cells expressing wt, kd, or m10FGFR3 were serum starved, activated with FGF1, and harvested at the times indicated. FGFR3 was phosphorylated for intact and cleaved wtFR3, as well as intact mFGFR3, but not kdFGFR3 (Figure 5E; representative blot). We next performed pulse-chase analysis on wt and m10FGFR3 in the presence of FGF1. Mutation of the stem region did not affect glycosylation of the intact receptor, although suppressing cleavage increased the half-life of the intact receptor, as anticipated (Figure 5F; graphical representation, Figure 5G). We next assayed the half-life of intact receptor that was biotin labeled at the PM. Unlike pulse-chase analysis, which assays the half-life for total receptor biogenesis and degradation, cell surface biotinylation specifically assays the half-life of the PM, signaling-competent receptor fraction. Serum-starved cells expressing wt and m10FGFR3 were cell surface biotinylated prior to FGF1 stimulation. Lysates were harvested, and biotinylated proteins were purified at the times indicated. Figure 5H shows that intact, surface-labeled m10FGFR3 persists significantly longer than intact, surface-labeled wtFGFR3. This is shown graphically in Figure 5I.

Cleaved FGFR3 is a substrate for γ-secretase proteolysis

As noted earlier, many transmembrane proteins that undergo ectodomain cleavage become substrates for subsequent intramembrane cleavage by γ-secretase, that is, RIP, yielding a soluble cytosolic fragment referred to as a soluble intracellular fragment (sICD). The hypothetical cleavage sites for FGFR3 are depicted in Figure 6A. Generally, such sICDs are labile and detected only in the presence of proteasome inhibitors (Jung *et al.*, 2003) such as epoxomicin and lactacystin. To determine whether FGFR3 is processed through the RIP pathway, we pulse labeled cells stably expressing wtFGFR3 and chased in the presence of FGF1 plus epoxomicin. A novel band migrating with slightly faster mobility than the ectodomain cleavage product was detected in the presence of the proteasome inhibitor (Figure 6B, lane E). Because of the linear nature of RIP, one would not expect to detect this novel band in the presence of γ-secretase inhibitors such as *N*-(*N*-(3,5-difluorophenacetyl)-L-alanyl)-*S*-phenylglycine *t*-butyl ester (DAPT) or compound E, even in the presence of a proteasome inhibitor. This expectation was validated as shown in Figure 6B, lanes D, GSI, and GSI/E. As implied, a major consequence of RIP is liberation of the sICD into the cytoplasm. Accordingly, we performed a related experiment, subjecting wtFGFR3-expressing cells to subcellular fractionation prior to Western blotting. As predicted, the novel fragment was detected in the cytosol of cells treated with the proteasome inhibitor lactacystin but not in cells treated with γ-secretase inhibitors (Figure 6C).

In some contexts RIP may promote degradation of membrane-anchored proteins (Kopan and Ilagan, 2004). Therefore we assessed the impact of cleavage on the stability of the FGFR3 and its cleavage products in the presence of inhibitors. Similar to other results (Alwan *et al.*, 2003; Laederich *et al*, 2011), proteasome inhibitors either stabilized or delayed degradation of intact FGFR3 (Figure 6D). More dramatically, γ-secretase and proteasome inhibitors significantly stabilized the S1- and S2-cleaved fragments. In some cases RIP may generate an sICD that functions independent of the intact receptor. Indeed, the sICD of several RIP substrates, including ErbB4, CSFR, Ryk, Met, and p75, have been reported to localize to the nucleus (Carpenter, 2003; Lyu *et al.*, 2008; Ancot *et al.*, 2009; Parkhurst *et al.*, 2010). Therefore we asked whether the same were true for FGFR3. Because only a minor portion of endogenous or stably expressed FGFR3 is detected as the sICD, 293T cells were made to transiently overexpress full-length, untagged wt and cleavage-resistant m10FGFR3, immunostained with a C-terminal FGFR3 antibody, and evaluated by confocal microscopy. Nuclear staining was observed in cells overexpressing wtFGFR3 (Figure 6E, top), whereas such staining was minimal in cells overexpressing m10FGFR3 (Figure 6E, middle). To better distinguish endogenous FGFR3 from the transfected receptor, we transiently expressed yellow fluorescent protein (YFP)–tagged FGFR3-sICD (YFP-sICD) to look for nuclear localization. YFP-sICD was detected in the nucleus as well as the cytoplasm, consistent with its ability to traffic to the nucleus (Figure 6E, bottom).

DISCUSSION

Our investigation reveals that FGFR3 undergoes RIP in response to activation at the cell surface, similar to several other RTKs. Unlike most RTKs, including what is known for FGFR1 and FGFR2, ligand-induced cleavage of FGFR3 requires dynamin/clathrin–mediated endocytosis of the intact receptor to an endosomal compartment where the initial, S1 cleavage is carried out. This cleavage event most likely involves an endosomal cathepsin rather than the ADAM 10/17 sheddases most commonly implicated in ectodomain shedding/cleavage. Our results suggest that S1 cleavage generates a labile ectodomain fragment and a membrane-anchored intracellular fragment that may be signaling competent and traffic independent of the intact receptor. Following S1 cleavage, FGFR3 is cleaved by γ-secretase (S2) to generate an sICD. Our observations, based primarily on FGF1-induced activation, suggest that cleavage influences the half-life of the intact receptor and generates a soluble fragment that can traffic to the nucleus. Although others have described ectodomain cleavage of FGFR3 and related FGFRs, our study is the first mechanistic investigation of this event and the first to demonstrate RIP of an FGFR.

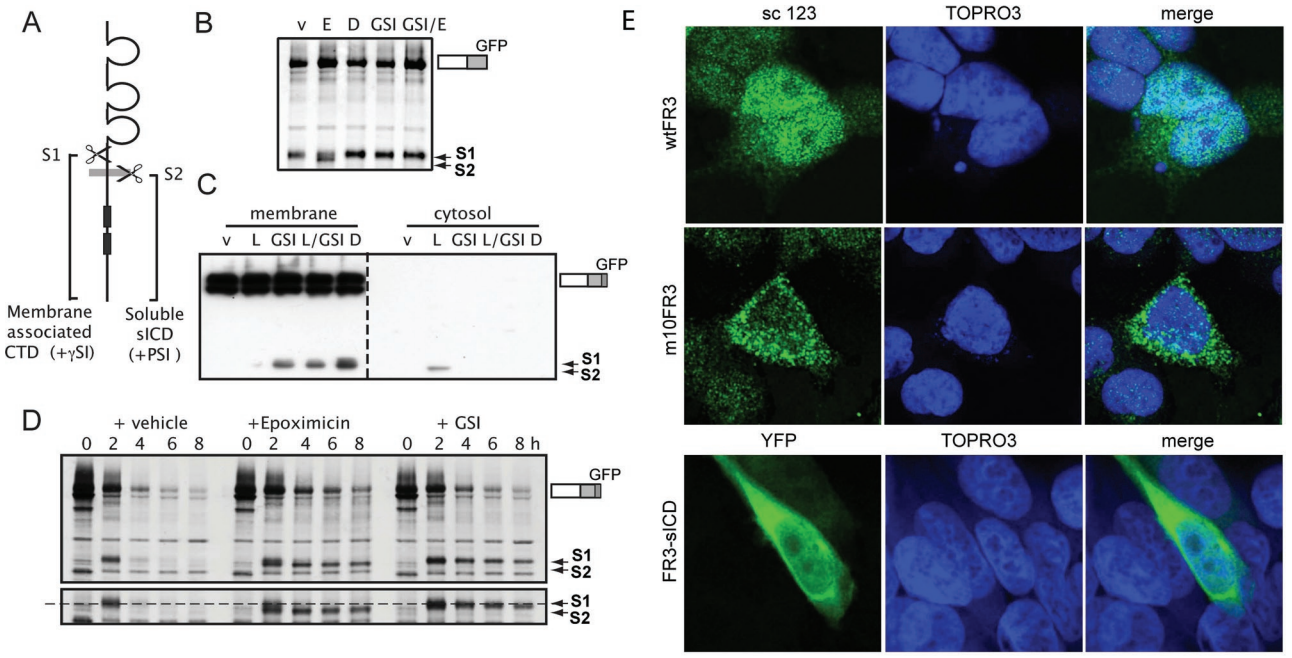

FIGURE 6: FGFR3 is cleaved by γ-secretase. (A) Cartoon of cleavage sites (S1, putative cathepsin; S2, γ-secretase) and their subcellular localization. γSI, γ-secretase inhibitor; PSI, proteasome inhibitor. (A) Cells expressing wtFR3-GFP were pulse labeled in the presence of FGF1 and then chased 2.5 h in the presence of inhibitors. D, 25 μM DAPT; E, 1 μM epoxomicin; GSI, 5 μM compound E; v, DMSO. (C) Western blot of cells expressing wtFR3-GFP, cultured 5 h in the presence of inhibitors, subject to subcellular fractionation, and probed for C-terminal GFP tag. Left, membrane-associated proteins; right, cytosolic proteins. L, 10 μM lactacystin. (D) Cells expressing wtFR3-GFP were pulse labeled and then chased in the presence of FGF1 plus inhibitors. Bottom, longer exposure to show the size shift of the cleaved fragment. Dashed line, S1-cleaved FR3. (E) Confocal images of cells transiently overexpressing untagged wtFR3 (top), m10FR3 (middle), or YFP-tagged FR3-sICD (bottom, YFP-sICD). sc 123, C-terminal anti-FGFR3 antibody (green); YFP pseudo-colored green; TOPRO3, nuclear stain (blue).

We did not identify a specific protease responsible for FGFR3 ectodomain cleavage, and there may be several reasons why. Notably, the requirement for endocytosis distinguishes FGFR3 proteolysis from that of most other RTKs, and although we used membrane-permeable protease inhibitors when available, we cannot exclude the possibility that they may not have been delivered to the cleavage compartment at levels sufficient to block proteolysis. In addition, most cleavage substrates are cleaved by more than one protease, depending on cell type and experimental conditions, and these proteases are often components of proteolytic cascades. Inhibition of one protease can positively or negatively influence related proteases and can result in activation of cryptic cleavage sites within a substrate (Overall and Blobel, 2007). Our results point to an endosomal cathepsin, and based on our inhibitor results, cathepsins B and L are prime candidates for cleaving FGFR3. An alternate candidate is cathepsin G, which has been implicated in the ectodomain shedding of CD43 (Mambole *et al.*, 2008), IL-6R (Bank *et al.*, 1999), and RANKL (Wilson *et al.*, 2008). However, preliminary experiments showed cleavage of FGFR3 was not inhibited in the presence of a cathepsin G inhibitor. Further studies to delineate the protease(s) responsible for cleavage of FGFR3 are underway, but they are beyond the scope of this initial investigation.

Mutagenesis of the LME and flanking stem region sequence was carried out to better understand the requirements for cleaving FGFR3. Deletions spanning the LME motif suppressed cleavage without negatively affecting receptor activation or trafficking. Of the mutants examined, only deletion of the 10 amino acids adjacent to the TMD (m10) fully suppressed cleavage, consistent with cleavage requiring a spatial or steric requirement as reported for several other juxtamembrane protease substrates (Migaki *et al.*, 1995; Deng *et al.*, 1996b). For example, reducing the stem region of ErbB4 from 23 amino acids (JM-a isoform) to 13 amino acids (JM-b isoform) is sufficient to repress receptor cleavage (Elenius *et al.*, 1997). The FGFR3IIIc stem region consists of 18 amino acids, and the IIIb isoform consists of 21 (UniProtKB). If cleavage of FGFR3 is regulated by stem length, then it is not unexpected that reducing the stem region to eight amino acids suppresses cleavage. Likewise, comparison of the cleavage sequence across species shows that although the LME sequence is conserved for mouse, chick, and rat, it is LVE for human and bovine. Cleavage of the human FGFR3 LVE motif was comparable to the mouse LME motif, providing additional support for the notion that cleavage is not sequence specific.

Our findings indicate that tyrosine phosphorylation of FGFR3 is necessary but not sufficient for FGF1-induced cleavage of FGFR3. It is unresolved whether phosphorylation regulates trafficking to the cleavage compartment, allows for recognition of FGFR3 as a cleavage substrate, or is required for activation of the receptor-specific protease. We anticipated cleavage to be regulated by the cellular context or the tissue/cell type in which it is expressed. Thus far only Chinese hamster ovary cells show a cleavage deficiency, although whether this results from a trafficking defect, rapid degradation of the ICD, or another mechanism is unknown. It is interesting to note both FGF1 and PMA reduce the amount of mature FGFR3 from serum-starved cells (Supplemental Figure S3B), either through degradation or regulated cleavage of the intact receptor. In other cells lines, however, we showed that cleavage depends on FGF concentration and correlates with the intensity of receptor phosphorylation. Because FGFRs are phosphorylated at multiple tyrosine sites, it is

possible that cleavage of FGFR3 requires an ordered, threshold level of phosphorylation; that is, receptors that are subject to only first- or second-phase phosphorylation events (Bae *et al.*, 2010) may not be cleaved. FGF2, FGF8, and FGF10 form morphogen gradients during embryogenesis (Kengaku and Okamoto, 1995; Miura *et al.*, 2009; Yu *et al.*, 2009; Toyoda *et al.*, 2010). If cleavage of FGFR3 depends on FGF concentration, then cleavage may provide a molecular switch to alter cellular responses to a gradient of FGF. Future studies will better define these activities, as well as the temporal/spatial requirements for cleavage of FGFR3.

Following the discovery of ErbB4 cleavage, more and more RTKs—in addition to other transmembrane proteins—have been found to undergo ectodomain cleavage, and many of these are also substrates for RIP. In some cases the biological consequence of cleavage is known; in most, it is not. For a small number of proteins, such as Notch (Kopan and Ilagan, 2009) and Toll-Like Receptor 9 (Park *et al.*, 2008), proteolytic cleavage is absolutely required for activity. For many receptors, ectodomain shedding at the PM releases an ECD capable of sequestering ligand and down-regulating signaling. Because ligand-induced cleavage of FGFR3 generates a labile ECD within an endosomal compartment, this effect seems unlikely. For other receptors, such as ErbB4 (Naresh *et al.*, 2006; Sardi *et al.*, 2006), Tie1 (Marron *et al.*, 2007), and TrkA (Cabrera *et al.*, 1996; Diaz-Rodriguez *et al.*, 1999), cleavage modifies their activity and subcellular localization, which appears to be the case for FGFR3.

One consequence of FGFR3 ectodomain cleavage may be to shorten the half-life of activated, surface-localized (biotinylated) receptor, possibly through attenuating its recycling or altering its transit through the endocytic/degradative pathway. Alternatively, production of the sICD may be the primary consequence of cleavage. FGFR3 has been found in the nucleus in several disease states (Johnston *et al.*, 1995; Zammit *et al.*, 2001), yet except for the finding of splice variants of FGFR3 that lack the TMD, mechanisms to promote this localization have not been forthcoming (Schlessinger and Lemmon, 2006). RIP provides one such mechanism (Ni *et al.*, 2001; Blobel *et al.*, 2009; Carpenter and Liao, 2009). Our findings raise the possibility that FGFR3 functions may be mediated through novel nuclear interactions in addition to the well-established kinase network pathways. They may be relevant to understanding the pathogenesis of diseases, such as achondroplasia and cancer, and potentially to their treatment. Further investigation will be needed to delineate the nature and significance of this possibility. Such studies are underway.

MATERIALS AND METHODS

Constructs and cell lines

Cos7 cell lines stably expressing C-terminally tagged wtFGFR3 and TDII were previously described (Cho *et al.*, 2004). FGFR3-GFP fusion proteins were excised from pEGFR-FGFR3-N3 as a *Hin*dIII/*Not*I fragment and subcloned into pcDNA5/FRT/TO (Invitrogen, Carlsbad, CA). FGFR3-V5 fusion proteins were excised from pcDNA6-FGFR3-V5His (version B) as a *Hin*dIII/*Pme*I fragment and subcloned into pcDNA5/FRT/TO. pcDNA5/FRT/TO constructs were recombined into T-Rex 293 cells (Invitrogen), per manufacturer's recommendation, to generate stable tet-inducible FGFR3 cell lines. FGFR3 constructs were also used to generate stable MEF cell lines; hygromycin-resistant clones were isolated and characterized for FGFR3 protein levels. Stem mutants (mFGFR3) were generated using q QuikChange Site-Directed Mutagenesis Kit (Stratagene, Santa Clara, CA), per manufacturer's instructions. pcDNA3.1(-) ErbB4-JMa/CYT2 was obtained from Graham Carpenter (Vanderbilt-Ingram Cancer Center, Vanderbilt University Medical Center, Nashville, TN). mCherry and mOrange were obtained from Roger Y. Tsien (Department of Pharmacology and Department of Chemistry and Biochemistry, University of California, San Diego, La Jolla, CA).

Reagents and antibodies

The following antibodies/stains were used: α-GFP: (IP) Abcam (Cambridge, MA) Ab290 and (IB) Clontech (Mountain View, CA) JL-8. α-V5: Invitrogen. α-FGFR3: Santa Cruz Biotechnology (Santa Cruz, CA) sc-123. TO-PRO3: Invitrogen. Alexa Fluor: Molecular Probes/Invitrogen. α-ErbB4: Epitomics (2218-1). Chemicals were purchased from Sigma-Aldrich (St. Louis, MO), with the following exceptions. Calbiochem (La Jolla, CA): AEBSF, aprotinin, cathepsin inhibitor I, CA-074 Me, DAPT, EST (E64d), GM6001, PD173074, and PMA. Enzo (Plymouth, PA): Compound E, epoxomicin, lactacystin, Z-FA-FMK. LC Laboratories (Woburn, MA): bafilomycin A_1. BioMol, Enzo: ionomycin. Thermo Scientific (Waltham, MA): Super Signal West Pico, EZ-link Sulfo-NHS-SS-Biotin, NeutrAvidin Gel. Roche (Indianapolis, IN): complete mini EDTA-free protease inhibitor cocktail tablets, Fugene 6. FGF2, FGF4, FGF9, and FGF18 were purchased from R&D (Minneapolis, MN). FGF1 was a very generous gift from Moosa Mohammadi (Department of Pharmacology, New York University School of Medicine, New York, NY). BB94 (batimastat) was a gift from Richard Kenagy (Center for Cardiovascular Biology and Regenerative Medicine, University of Washington, Seattle, WA). Dynasore was a gift from Tom Kirchhausen (CBR Institute for Biomedical Research, Harvard Medical School/CBR, Boston, MA). Marimastat was a generous gift from Christopher Overall (Centre for Blood Research, University of British Columbia, Vancouver, Canada).

Cell culture

Cell lines were cultured in DMEM containing 10% fetal bovine serum (FBS) and the following additions: 100 μg/ml hygromycin B for stable Cos7 cell lines, 150 μg/ml hygromycin B plus 10 μg/ml blasticidin for stable T-Rex 293 lines, and 200 μg/ml hygromycin B for stable MEF lines. Stable Chinese hamster ovary lines were cultured in F12 media containing 10% FBS and 150 μg/ml hygromycin B. The prechondrocytic cell line TMC23 (a gift from Chi Xu, Division of Endocrinology and Metabolism, University of Texas Health Science Center at San Antonio, San Antonio, TX) was grown in DMEM plus 10% FBS (Xu *et al.*, 1998). For growth conditions cells were cultured in DMEM plus 10% FBS (growth media). To serum arrest cells, T-Rex 293 stable lines were tet induced (1 μg/ml) for 8 h in growth media, then serum starved overnight in DMEM containing 0.1% FBS depleted over a heparin column (DMEM/FBS(−)) plus tet. FGFR3 was then activated with DMEM/FBS(−) containing 20 ng/ml FGF1 and 3 U/ml heparin, unless stated otherwise. To assay for cleavage, T-Rex 293–stable lines were plated overnight in growth media lacking tet, then tet- induced for 8 h in DMEM/FBS(–) containing FGF1; stable MEF cells were serum starved overnight in DMEM/FBS(–) and then activated with FGF1. For drug studies, T-Rex–stable cell lines were cultured overnight, then tet induced 2 h in DMEM/FBS(–) containing FGF1 before inhibitors were added. Lysates were harvested 8 h later. For temperature block, Cos7 cells stably expressing wtFGFR3-GFP were incubated 5 h at 37 or 23°C in growth media.

Membrane fractionation

A crude subcellular fractionation was carried out as described by Holden and Horton (2009). Simply, washed cells were permeabilized with digitonin (50 mM 4-(2-hydroxyethyl)-1-piperazineethanesulfonic acid (HEPES), pH 7.4, 100 mM potassium acetate, 2.5 mM magnesium acetate, 150 μg/ml digitonin) and washed with digitonin (to remove cytosolic proteins), and the remaining material was lysed in

NP40 lysis buffer (50 mM Tris, pH 8.0, 150 mM NaCl, 1% NP40) containing Complete Protease Inhibitor tablets (Roche). Nuclei were pelleted by centrifugation (10 min, 6500 × *g*), and the solubilized membrane fraction was retained. Replica samples of whole-cell lysates were solubilized directly in RIPA buffer (150 mM NaCl, 50 mM Tris, pH 7.4, 1% Triton X-100, 1% deoxycholate, 0.05% SDS + Complete Protease Inhibitor tablets).

Immunoprecipitations and Western blots

For Western blots, cells were lysed in RIPA buffer and the lysates were clarified by centrifugation. Equal micrograms of lysate were separated by SDS–PAGE and transferred to polyvinylidene fluoride (PVDF) membranes, and the membranes (blocked in TBS-T [20 mM Tris, pH 7.5, 150 mM NaCl, 0.1% Tween 20] containing 5% BSA) were incubated overnight with primary antibodies in TBS-T containing 3% BSA. Washed membranes were probed with the appropriate anti–horseradish peroxidase secondary antibody (1:10,000) and detected using Super Signal West Pico, according to the manufacturer's recommendation. Chemiluminescence was detected by autoradiography. To assay for receptor phosphorylation, cells were serum starved overnight, then treated with growth factor for the times indicated. Cells were lysed in RIPA buffer containing Phosphatase Inhibitor Cocktail 2 (Sigma-Aldrich), and the lysates were clarified as described earlier. GFP antibody (0.13 µg ab290) was added to 200 µg of lysate and immunoprecipitated overnight using 20 µl of a 50% slurry of protein A agarose beads. Beads were washed four times in lysis buffer and boiled in Laemmli buffer (30% glycerol, 2.8% SDS, 0.2 M Tris, pH 6.8, 100 mM DTT, bromophenol blue). Immunoprecipitants were electrophoresed on 4–12% Tris/Bis Novex gels (Invitrogen), transferred to PVDF membranes, and blotted as described earlier.

Pulse-chase analysis

Cells were plated at 80% confluence and cultured overnight in growth media containing 1 µg/ml tet (carried throughout for T-Rex 293) or not (Cos7, TMC23). Cells were for pretreated 15 min in DMEM (–methionine/cysteine) containing 10% dialyzed FBS and then pulse labeled for 45 min (90 min for TMC23 cells) in DMEM (–methionine/cysteine) containing 10% dialyzed FBS plus 100 µCi/ml [^{35}S]methionine. Cells were washed and cultured in DMEM containing 10% FBS (or DMEM/FBS(–)/FGF1, as indicated) plus excess methionine/cysteine for the times indicated. Cells were lysed for 20 min in RIPA buffer; clarified lysates were immunoprecipitated overnight with 0.13 µg ab290, washed, and electrophoresed as described earlier. Gels were dried and subjected to autoradiography; scanned films were analyzed by densitometry using ImageJ (National Institutes of Health, Bethesda, MD).

Immunofluorescence

Primary mouse chondrocytes were electroporated with plasmid encoding V5-FGFR3-GFP using the AMAXA system, according to the manufacturer's recommendation (chondrocyte prep), and then plated onto coverslips overnight in growth media. Cos7 cells were plated onto coverslips, transfected with plasmid encoding V5-FGFR3-GFP using Fugene 6 (according to the manufacturer's recommendation), and cultured overnight in growth media. Cells were fixed for 20 min in 4% PFA, permeabilized for 20 min using ice-cold methanol, and blocked in phosphate-buffered saline (PBS) containing 10% goat serum. Anti-V5 antibody was added (1:1000 in PBS containing 0.1% goat serum) overnight at 4°C. Coverslips were probed 1 h with Alexa 543 (1:400) secondary antibody, washed, and air dried. Coverslips were mounted with Permount and imaged using a Leica TCS SP2 (Wetzlar, Germany) laser scanning confocal system mounted on a DM IRE2 inverted microscope using a 63× water-immersion objective. Confocal slices of fixed cells were imaged sequentially for C-terminal GFP and ECD V5–Alexa 543 fluorescence; imaged stacks were compiled using Image5D (ImageJ). To detect V5-tagged FGFR3 ECD that had been endocytosed, stable T-Rex 293 lines expressing FGFR3(V5)-GFP were plated onto coverslips in the presence of tet, serum-starved overnight using DMEM/FBS(–) media, incubated with anti-V5 antibodies (1:1000) at 4°C, washed (to remove unbound antibody), and then stimulated with FGF1 for the times indicated. Cells were fixed, permeabilized, and stained with Alexa 543 (1:400) secondary antibody as described previously. For nuclear localization of FGFR3, 293 cells were plated onto poly-L-lysine–treated coverslips; transient transfections were performed using Fugene 6, cotransfecting untagged wt, m10, or FGFR3-sICD plus 1/10 concentration of mCherry, to mark transfected cells. Cells were fixed, permeabilized using 0.2% Triton X-100 in PBS, and blocked as described. sc-123 (FGFR3 antibody) was added at 1:500 overnight in 0.5% goat serum; cells were washed and probed 1 h with Alexa 488 (1:400) secondary antibody plus TO-PRO3 iodine (1:500) in 0.5% goat serum. Cells were washed, mounted, and imaged as described earlier.

Cell surface biotinylation/endocytosis assays

Cell surface biotinylations were performed per manufacturer's recommendation. Briefly, serum-starved cells were cultured as indicated, placed on ice, washed in PBS, and treated for 20 min with 250 µg/ml EZ-link Sulfo-NHS-SS-biotin at 4°C. Excess reagent was quenched using 1.86 mg/ml glycine/PBS, washed in Tris-buffered saline (TBS: 25 mM Tris, pH 7.2, 150 mM NaCl), and lysed in RIPA buffer. Equal micrograms of lysate were precipitated for 1 h using NeutrAvidin Gel. The NeutrAvidin Gel was washed three times in lysis buffer and biotin-labeled proteins eluted into Laemmli buffer containing 100 mM DTT. Endocytosis assays were performed as described (Fabbri *et al.*, 1999), with the following modifications. Serum-starved cells were labeled for 20 min with 250 µg/ml EZ-link Sulfo-NHS-SS-biotin at 4°C, washed with PBS, and then incubated at 37°C in prewarmed DMEM/FBS(–) containing FGF1 for the times indicated. Cells were returned to ice and treated 2× 20 min with ice-cold glutathione (GSH; membrane-impermeable reducing agent: 75 mM NaCl, 1 mM EDTA, 50 mM glutathione, supplemented with 0.1% BSA and 75 mM NaOH just prior to use) to remove cell surface biotinylated groups; endocytosed proteins retain the biotin residues. Cells were treated with 0.192 M glycine in 25 mM Tris-HCl, pH 7.4, to quench free sulfo-reactive groups, washed twice in TBS, and lysed in RIPA buffer. Equal micrograms of lysate were purified as described earlier; equal volumes of NeutrAvidin-purified protein were evaluated by Western blot. For graphical analysis, at least three independent experiments were scanned and analyzed by densitometry using ImageJ. Time points were represented as the percentage of the initial biotinylated protein; the arithmetic mean and SD were calculated for each time point.

ACKNOWLEDGMENTS

We thank Linda Musil (Oregon Health and Sciences University) for her scientific contributions and critical review of the manuscript. We also thank Jesse Vance (Shriners Hospital for Children, Portland, OR) for N-terminal sequencing of cleaved FGFR3. This research was supported by research and fellowship training grants from the Shriners Research Program. C.R.D. was awarded a Shriners Research Fellowship Grant.

REFERENCES

Alwan HA, van Zoelen EJ, van Leeuwen JE (2003). Ligand-induced lysosomal epidermal growth factor receptor (EGFR) degradation is preceded by proteasome-dependent EGFR de-ubiquitination. J Biol Chem 278, 35781–35790.

Ancot F, Foveau B, Lefebvre J, Leroy C, Tulasne D (2009). Proteolytic cleavages give receptor tyrosine kinases the gift of ubiquity. Oncogene 28, 2185–2195.

Bae JH, Boggon TJ, Tome F, Mandiyan V, Lax I, Schlessinger J (2010). Asymmetric receptor contact is required for tyrosine autophosphorylation of fibroblast growth factor receptor in living cells. Proc Natl Acad Sci USA 107, 2866–2871.

Bank U, Reinhold D, Schneemilch C, Kunz D, Synowitz HJ, Ansorge S (1999). Selective proteolytic cleavage of IL-2 receptor and IL-6 receptor ligand binding chains by neutrophil-derived serine proteases at foci of inflammation. J Interferon Cytokine Res 19, 1277–1287.

Belleudi F, Leone L, Nobili V, Raffa S, Francescangeli F, Maggio M, Morrone S, Marchese C, Torrisi MR (2007). Keratinocyte growth factor receptor ligands target the receptor to different intracellular pathways. Traffic 8, 1854–1872.

Bernard-Pierrot I *et al.* (2006). Oncogenic properties of the mutated forms of fibroblast growth factor receptor 3b. Carcinogenesis 27, 740–747.

Blobel CP, Carpenter G, Freeman M (2009). The role of protease activity in ErbB biology. Exp Cell Res 315, 671–682.

Brown MS, Ye J, Rawson RB, Goldstein JL (2000). Regulated intramembrane proteolysis: a control mechanism conserved from bacteria to humans. Cell 100, 391–398.

Burke D, Wilkes D, Blundell TL, Malcolm S (1998). Fibroblast growth factor receptors: lessons from the genes. Trends Biochem Sci 23, 59–62.

Cabrera N, Diaz-Rodriguez E, Becker E, Martin-Zanca D, Pandiella A (1996). TrkA receptor ectodomain cleavage generates a tyrosine-phosphorylated cell-associated fragment. J Cell Biol 132, 427–436.

Cappellen D, De Oliveira C, Ricol D, de Medina S, Bourdin J, Sastre-Garau X, Chopin D, Thiery JP, Radvanyi F (1999). Frequent activating mutations of FGFR3 in human bladder and cervix carcinomas. Nat Genet 23, 18–20.

Carpenter G (2003). Nuclear localization and possible functions of receptor tyrosine kinases. Curr Opin Cell Biol 15, 143–148.

Carpenter G, Liao HJ (2009). Trafficking of receptor tyrosine kinases to the nucleus. Exp Cell Res 315, 1556–1566.

Chaffer CL, Dopheide B, Savagner P, Thompson EW, Williams ED (2007). Aberrant fibroblast growth factor receptor signaling in bladder and other cancers. Differentiation 75, 831–842.

Chesi M, Nardini E, Brents LA, Schröck E, Ried T, Kuehl WM, Bergsagel PL (1997). Frequent translocation t(4;14)(p16.3;q32.3) in multiple myeloma is associated with increased expression and activating mutations of fibroblast growth factor receptor 3. Nat Genet 16, 260–264.

Cho JY, Guo C, Torello M, Lunstrum GP, Iwata T, Deng C, Horton WA (2004). Defective lysosomal targeting of activated fibroblast growth factor receptor 3 in achondroplasia. Proc Natl Acad Sci USA 101, 609–614.

Colvin JS, Bohne BA, Harding GW, McEwen DG, Ornitz DM (1996). Skeletal overgrowth and deafness in mice lacking fibroblast growth factor receptor 3. Nat Genet 12, 390–397.

Dailey L, Ambrosetti D, Mansukhani A, Basilico C (2005). Mechanisms underlying differential responses to FGF signaling. Cytokine Growth Factor Rev 16, 233–247.

de Oca PM, Malarde V, Proust R, Dautry-Varsat A, Gesbert F (2010). Ectodomain shedding of interleukin-2 receptor beta and generation of an intracellular functional fragment. J Biol Chem 285, 22050–22058.

Deng C, Wynshaw-Boris A, Zhou F, Kuo A, Leder P (1996a). Fibroblast growth factor receptor 3 is a negative regulator of bone growth. Cell 84, 911–921.

Deng P, Rettenmier CW, Pattengale PK (1996b). Structural requirements for the ectodomain cleavage of human cell surface macrophage colony-stimulating factor. J Biol Chem 271, 16338–16343.

Diaz-Rodriguez E, Cabrera N, Esparis-Ogando A, Montero JC, Pandiella A (1999). Cleavage of the TrkA neurotrophin receptor by multiple metalloproteases generates signalling-competent truncated forms. Eur J Neurosci 11, 1421–1430.

Elenius K, Corfas G, Paul S, Choi CJ, Rio C, Plowman GD, Klagsbrun M (1997). A novel juxtamembrane domain isoform of HER4/ErbB4Isoform-specific tissue distribution and differential processing in response to phorbol ester. J Biol Chem 272, 26761–26768.

Fabbri M, Fumagalli L, Bossi G, Bianchi E, Bender JR, Pardi R (1999). A tyrosine-based sorting signal in the beta2 integrin cytoplasmic domain mediates its recycling to the plasma membrane and is required for ligand-supported migration. EMBO J 18, 4915–4925.

Hadland BK, Huppert SS, Kanungo J, Xue Y, Jiang R, Gridley T, Conlon RA, Cheng AM, Kopan R, Longmore GD (2004). A requirement for Notch1 distinguishes 2 phases of definitive hematopoiesis during development. Blood 104, 3097–3105.

Hanneken A (2001). Structural characterization of the circulating soluble FGF receptors reveals multiple isoforms generated by secretion and ectodomain shedding. FEBS Lett 489, 176–181.

Holden P, Horton WA (2009). Crude subcellular fractionation of cultured mammalian cell lines. BMC Res Notes 2, 243.

Idkowiak-Baldys J, Becker KP, Kitatani K, Hannun YA (2006). Dynamic sequestration of the recycling compartment by classical protein kinase C. J Biol Chem 281, 22321–22331.

Johnston CL, Cox HC, Gomm JJ, Coombes RC (1995). Fibroblast growth factor receptors (FGFRs) localize in different cellular compartments. A splice variant of FGFR-3 localizes to the nucleus. J Biol Chem 270, 30643–30650.

Jung KM, Tan S, Landman N, Petrova K, Murray S, Lewis R, Kim PK, Kim DS, Ryu SH, Chao MV (2003). Regulated intramembrane proteolysis of the p75 neurotrophin receptor modulates its association with the TrkA receptor. J Biol Chem 278, 42161–42169.

Kengaku M, Okamoto H (1995). bFGF as a possible morphogen for the anteroposterior axis of the central nervous system in *Xenopus*. Development 121, 3121–3130.

Kopan R, Ilagan MX (2004). Gamma-secretase: proteasome of the membrane? Nat Rev Mol Cell Biol 5, 499–504.

Kopan R, Ilagan MXG (2009). The canonical Notch signaling pathway: unfolding the activation mechanism. Cell 137, 216–233.

Laederich MB, Degnin CR, Lunstrum GP, Horton WA (2011). Fibroblast growth factor receptor 3 (FGFR3) is a strong heat shock protein 90 (Hsp90) client: implications for therapeutic manipulation. J Biol Chem 286, 19597–19604.

Lal M, Caplan M (2011). Regulated intramembrane proteolysis: signaling pathways and biological functions. Physiology 26, 34–44.

Levi E, Fridman R, Miao HQ, Ma YS, Yayon A, Vlodavsky I (1996). Matrix metalloproteinase 2 releases active soluble ectodomain of fibroblast growth factor receptor 1. Proc Natl Acad Sci USA 93, 7069–7074.

Lievens PM-J, Liboi E (2003). The thanatophoric dysplasia type II mutation hampers complete maturation of fibroblast growth factor receptor 3 (FGFR3), which activates signal transducer and activator of transcription 1 (STAT1) from the endoplasmic reticulum. J Biol Chem 278, 17344–17349.

Linggi B, Cheng QC, Rao AR, Carpenter G (2006). The ErbB-4 s80 intracellular domain is a constitutively active tyrosine kinase. Oncogene 25, 160–163.

Lyu J, Yamamoto V, Lu W (2008). Cleavage of the Wnt receptor Ryk regulates neuronal differentiation during cortical neurogenesis. Dev Cell 15, 773–780.

Macia E, Ehrlich M, Massol R, Boucrot E, Brunner C, Kirchhausen T (2006). Dynasore, a cell-permeable inhibitor of dynamin. Dev Cell 10, 839–850.

Mambole A, Baruch D, Nusbaum P, Bigot S, Suzuki M, Lesavre P, Fukuda M, Halbwachs-Mecarelli L (2008). The cleavage of neutrophil leukosialin (CD43) by cathepsin G releases its extracellular domain and triggers its intramembrane proteolysis by presenilin/gamma-secretase. J Biol Chem 283, 23627–23635.

Maretzky T, Yang G, Ouerfelli O, Overall CM, Worpenberg S, Hassiepen U, Eder J, Blobel CP (2009). Characterization of the catalytic activity of the membrane-anchored metalloproteinase ADAM15 in cell-based assays. Biochem J 420, 105–113.

Marron MB, Singh H, Tahir TA, Kavumkal J, Kim HZ, Koh GY, Brindle NP (2007). Regulated proteolytic processing of Tie1 modulates ligand responsiveness of the receptor-tyrosine kinase Tie2. J Biol Chem 282, 30509–30517.

Matthews V *et al.* (2003). Cellular cholesterol depletion triggers shedding of the human interleukin-6 receptor by ADAM10 and ADAM17 (TACE). J Biol Chem 278, 38829–38839.

Migaki GI, Kahn J, Kishimoto TK (1995). Mutational analysis of the membrane-proximal cleavage site of L-selectin: relaxed sequence specificity surrounding the cleavage site. J Exp Med 182, 549–557.

Miura T, Hartmann D, Kinboshi M, Komada M, Ishibashi M, Shiota K (2009). The cyst-branch difference in developing chick lung results from a different morphogen diffusion coefficient. Mech Dev 126, 160–172.

Monsonego-Ornan E, Adar R, Rom E, Yayon A (2002). FGF receptors ubiquitylation: dependence on tyrosine kinase activity and role in downregulation. FEBS Lett 528, 83–89.

Naresh A, Long W, Vidal GA, Wimley WC, Marrero L, Sartor CI, Tovey S, Cooke TG, Bartlett JM, Jones FE (2006). The ERBB4/HER4 intracellular domain 4ICD is a BH3-only protein promoting apoptosis of breast cancer cells. Cancer Res 66, 6412–6420.
Ni CY, Murphy MP, Golde TE, Carpenter G (2001). gamma-Secretase cleavage and nuclear localization of ErbB-4 receptor tyrosine kinase. Science 294, 2179–2181.
Overall CM, Blobel CP (2007). In search of partners: linking extracellular proteases to substrates. Nat Rev Mol Cell Biol 8, 245–257.
Pandit SG, Govindraj P, Sasse J, Neame PJ, Hassell JR (2002). The fibroblast growth factor receptor, FGFR3, forms gradients of intact and degraded protein across the growth plate of developing bovine ribs. Biochem J 361, 231–241.
Park B, Brinkmann MM, Spooner E, Lee CC, Kim Y-M, Ploegh HL (2008). Proteolytic cleavage in an endolysosomal compartment is required for activation of Toll-like receptor 9. Nat Immunol 9, 1407–1414.
Parkhurst CN, Zampieri N, Chao MV (2010). Nuclear localization of the p75 neurotrophin receptor intracellular domain. J Biol Chem 285, 5361–5368.
Peduto L, Reuter VE, Shaffer DR, Scher HI, Blobel CP (2005). Critical function for ADAM9 in mouse prostate cancer. Cancer Res 65, 9312–9319.
Pozner-Moulis S, Pappas DJ, Rimm DL (2006). Met, the hepatocyte growth factor receptor, localizes to the nucleus in cells at low density. Cancer Res 66, 7976–7982.
Richelda R *et al*. (1997). A novel chromosomal translocation t(4; 14)(p16.3; q32) in multiple myeloma involves the fibroblast growth-factor receptor 3 gene. Blood 90, 4062–4070.
Rousseau F, Bonaventure J, Legeai-Mallet L, Pelet A, Rozet JM, Maroteaux P, Le Merrer M, Munnich A (1996a). Mutations of the fibroblast growth factor receptor-3 gene in achondroplasia. Horm Res 45, 108–110.
Rousseau F, el Ghouzzi V, Delezoide AL, Legeai-Mallet L, Le Merrer M, Munnich A, Bonaventure J (1996b). Missense FGFR3 mutations create cysteine residues in thanatophoric dwarfism type I (TD1). Hum Mol Genet 5, 509–512.
Rutledge EA, Green FA, Enns CA (1994). Generation of the soluble transferrin receptor requires cycling through an endosomal compartment. J Biol Chem 269, 31864–31868.
Sardi SP, Murtie J, Koirala S, Patten BA, Corfas G (2006). Presenilin-dependent ErbB4 nuclear signaling regulates the timing of astrogenesis in the developing brain. Cell 127, 185–197.
Schlessinger J, Lemmon MA (2006). Nuclear signaling by receptor tyrosine kinases: the first robin of spring. Cell 127, 45–48.
Schnitzer JE, Oh P, Pinney E, Allard J (1994). Filipin-sensitive caveolae-mediated transport in endothelium: reduced transcytosis, scavenger endocytosis, and capillary permeability of select macromolecules. J Cell Biol 127, 1217–1232.
Shah S, Lee SF, Tabuchi K, Hao YH, Yu C, LaPlant Q, Ball H, Dann CE 3rd, Sudhof T, Yu G (2005). Nicastrin functions as a gamma-secretase-substrate receptor. Cell 122, 435–447.
Shiang R, Thompson LM, Zhu YZ, Church DM, Fielder TJ, Bocian M, Winokur ST, Wasmuth JJ (1994). Mutations in the transmembrane domain of FGFR3 cause the most common genetic form of dwarfism, achondroplasia. Cell 78, 335–342.
Tavormina PL, Shiang R, Thompson LM, Zhu YZ, Wilkin DJ, Lachman RS, Wilcox WR, Rimoin DL, Cohn DH, Wasmuth JJ (1995). Thanatophoric dysplasia (types I and II) caused by distinct mutations in fibroblast growth factor receptor 3. Nat Genet 9, 321–328.
Toyoda R, Assimacopoulos S, Wilcoxon J, Taylor A, Feldman P, Suzuki-Hirano A, Shimogori T, Grove EA (2010). FGF8 acts as a classic diffusible morphogen to pattern the neocortex. Development 137, 3439–3448.
Trudel S, Ely S, Farooqi Y, Affer M, Robbiani DF, Chesi M, Bergsagel PL (2004). Inhibition of fibroblast growth factor receptor 3 induces differentiation and apoptosis in t(4;14) myeloma. Blood 103, 3521–3528.
Vecchi M, Baulida J, Carpenter G (1996). Selective cleavage of the heregulin receptor ErbB-4 by protein kinase C activation. J Biol Chem 271, 18989–18995.
Vecchi M, Carpenter G (1997). Constitutive proteolysis of the ErbB-4 receptor tyrosine kinase by a unique, sequential mechanism. J Cell Biol 139, 995–1003.
von Tresckow B, Kallen KJ, von Strandmann EP, Borchmann P, Lange H, Engert A, Hansen HP (2004). Depletion of cellular cholesterol and lipid rafts increases shedding of CD30. J Immunol 172, 4324–4331.
Webster MK, Donoghue DJ (1996). Constitutive activation of fibroblast growth factor receptor 3 by the transmembrane domain point mutation found in achondroplasia. EMBO J 15, 520–527.
Webster MK, Donoghue DJ (1997). FGFR activation in skeletal disorders: too much of a good thing. Trends Genet 13, 178–182.
Williams CC, Allison JG, Vidal GA, Burow ME, Beckman BS, Marrero L, Jones FE (2004). The ERBB4/HER4 receptor tyrosine kinase regulates gene expression by functioning as a STAT5A nuclear chaperone. J Cell Biol 167, 469–478.
Wilson TJ, Nannuru KC, Futakuchi M, Sadanandam A, Singh RK (2008). Cathepsin G enhances mammary tumor-induced osteolysis by generating soluble receptor activator of nuclear factor-kappaB ligand. Cancer Res 68, 5803–5811.
Wolfe MS (2009). gamma-Secretase in biology and medicine. Semin Cell Dev Biol 20, 219–224.
Xu C, Ji X, Harris MA, Mundy GR, Harris SE (1998). A clonal chondrocytic cell line derived from BMP-2/T antigen-expressing transgenic mouse. In Vitro Cell Dev Biol Anim 34, 359–363.
Yu SR, Burkhardt M, Nowak M, Ries J, Petrasek Z, Scholpp S, Schwille P, Brand M (2009). Fgf8 morphogen gradient forms by a source-sink mechanism with freely diffusing molecules. Nature 461, 533–536.
Zammit C, Barnard R, Gomm J, Coope R, Shousha S, Coombes C, Johnston C (2001). Altered intracellular localization of fibroblast growth factor receptor 3 in human breast cancer. J Pathol 194, 27–34.
Zhou W, Carpenter G (2000). Heregulin-dependent trafficking and cleavage of ErbB-4. J Biol Chem 275, 34737–34743.